BUILD SIMUL (2012) 5: 51 – 60
DOI 10.1007/s12273-012-0068-5

Numerical study of the lock-up phenomenon of human exhaled droplets under a displacement ventilated room

Naiping Gao[1] (✉), Qibin He[2], Jianlei Niu[3]

1. Institute of Refrigeration and Thermal Engineering, School of Mechanical Engineering, Tongji University, 1239# Siping Road, Shanghai, China
2. Shenzhen Institute of Building Research, 29#, three Road, Meiao, Shangmeilin, Shenzhen, China
3. Department of Building Services Engineering, The Hong Kong Polytechnic University, Hung Hom, Kowloon, Hong Kong, China

Abstract

This paper adopts an Eulerian-Lagrangian approach to investigate the lock-up phenomenon (or trap phenomenon) of human exhaled droplets in a typical office room under displacement ventilation (DV). A particle-source-in-cell (PSI-C) scheme is used to correlate the concentration with the Lagrangian particle trajectories in computational cells. Respiratory droplets with sizes of 0.8 μm, 5 μm and 16 μm are released from a numerical thermal manikin (NTM). The influence factors including indoor temperature gradient, heat source configuration and exhalation modes are studied. It is found that large temperature gradient would result in trap phenomenon of small exhaled droplets (smaller than 5 μm). The intensive heat source near the NTM could help to transport the small droplets to the upper zone and decrease the concentration level in the trapped zone. Both nose-exhaled and mouth-exhaled small droplets would be trapped at the breathing height when temperature gradient is sufficiently high. However, the trap height of the droplets from mouth is a little bit higher. Because of large gravitational force, it is difficult for the thermal plume to carry 16 μm respiratory droplets to the upper zone.

Keywords

displacement ventilation,
human exhaled droplets,
thermal plume,
trap phenomenon,
Lagrangian simulation

Article History

Received: 12 December 2011
Revised: 15 January 2012
Accepted: 2 February 2012

1 Introduction

Human exhaled droplets may act as an agent of infectious diseases. The airborne transmission route of infectious diseases through respiratory droplets in enclosed environments was reported by Han et al. (2009), Mangili and Gendreau (2005) and Wagner et al. (2009). Displacement ventilation (DV) is one of the thermally stratified systems where temperature gradient is created. If the heat sources are also the gaseous contaminant sources, the contaminants will be transported to the upper level of the room by buoyant forces, and therefore guarantee a better ventilation efficiency than mixing ventilation (Bjorn and Nielsen 1996, 2002).

Some recent work has been carried out to assess the dispersion of exhaled particle/droplet in indoor environment. Chen and Zhao (2010) answered some key questions on dispersion of human exhaled droplets by numerical simulations and clarified the effect of evaporation, ventilation rate, ventilation pattern, relative humidity, temperature level, initial exhaled velocity, and droplet nuclei size on the transport of droplets. Seepana and Lai (2012) measured and modeled the temporal and spatial distribution of sneezed droplets in a full-scale chamber. The normalized peak concentrations in the breathing height in DV were higher than in mixing ventilation (MV). They attributed it to thermal stratification, room size and high sneezing velocity. Mui et al. (2009) compared the interpersonal exposure in DV and MV. For one sneezing process, the time integral exposure in DV is 2.5 times of that in MV for face-to-face scenario.

As to the indoor environment with vertical temperature gradient such as in displacement ventilation, previous studies demonstrate that at certain conditions human exhaled pollutants would be trapped or locked at the breathing height due to the temperature stratification. Skistad et al. (2004) believed that if the heat source was too weak, the plume might disintegrate at a certain level due to a stronger heat plume nearby. Then the contaminants would be trapped at this level and be slowly transported indirectly by the stronger

E-mail: gaonaiping@tongji.edu.cn

List of symbols

$\overline{C_j}$	particle concentration in the jth cell (μg/m^3)	$\boldsymbol{U}$	air velocity vector (m/s)
C_D	drag coefficient	u	air velocity (m/s)
$dt_{(i,j)}$	particle residence time of the ith trajectory in the jth cell (s)	u_p	particle velocity (m/s)
		u'	fluctuating velocity (m/s)
F_a	additional forces acting on the particles (m/s^2)	$\sqrt{\overline{u'^2}}$	local root-mean-square (RMS) value of the velocity fluctuations (m/s)
g	acceleration of gravity (m/s^2)		
k	the turbulence kinetic energy (m^2/s^2)	V_j	the volume of the jth cell (m^3)
$\dot{M}$	number or mass flow rate of each trajectory (μg/s per trajectory)	Γ_ϕ	effective diffusion coefficient
		ρ	air density (kg/m^3)
Re_p	particle Reynolds number	ρ_p	density of the particle material (kg/m^3)
S_ϕ	source term of the general form in the governing equation	ζ	normally distributed random number
		τ	particle relaxation time (s)
t	time (s)	ϕ	transport variable in the general governing equation

convection flows to the upper zone. Bjorn and Nielsen (2002) found that air exhaled through the mouth of a breathing manikin can be locked in a thermally stratified layer, where concentrations several times the exhaust one can occur. They concluded that if the vertical temperature gradient was larger than approximately 0.4–0.5℃/m, the trap layer can settle in breathing height. But they found this phenomenon disappeared when air was exhaled through the nose of the manikin. Qian et al. (2006) found that a high concentration layer of exhaled droplet nuclei (represented by gaseous pollutants) from a bed-lying manikin was observed within displacement ventilation. Gao et al. (2008) investigated exhaled droplets (0.1–10 μm in diameter) under DV systems and found that there was a lock-up layer of droplets in the breathing zone when droplets were exhaled from the human nose. More recently, Nielsen et al. (2012) showed the exposure increased up to 12 times the level of a fully mixed situation in a face-to-face case when the distance between manikins was 35 cm, and more than 2 times when 80 cm. It is serious setback resulting from the lock-up layer with respect to the protection against cross-infection. These studies all prove a characteristic of maximum concentrations in the middle height, which is different from the traditional thought of two-zone distribution of pollutants.

The only way for the contaminants to transport from the lower zone to upper zone in DV is via the plumes when the contaminants are released without momentum (Li et al. 2011). The thermal plumes of the human body and heat sources nearby play an important role in the distribution of exhaled contaminants. The exhalation airflow with weak buoyancy makes the distribution of exhaled contaminants differ from those released from heat sources without initial momentum. Moreover, the diameters of the exhaled droplets could be in the range of 0.1 μm to 1000 μm and rapidly shrink by approximately 50% when exposed to the air by evaporation (Chao et al. 2009; Morawska et al. 2009; Nicas et al. 2005). The transport behaviors of large droplets are different from those of small droplets and gaseous contaminants due to the relatively large gravity and drag force. Therefore, the influence of the above factors to the dispersion behaviors of respiratory droplets in DV requires to be fully explored and the parametric study of the trap phenomenon is really necessary.

This paper complements the previous studies on the lock-up effect by using an Eulerian-Lagrangian approach. The Eulerian-Lagrangian approach is one of the most popular simulation methods to study the droplet transport indoors (Chao and Wan 2006; Chao et al. 2008; Zhao et al. 2004). It treats the flow field as continues phase and assumes the particle as discrete phase. A particle-source-in-cell (PSI-C) scheme is used to correlate the concentration with the Lagrangian particle trajectories in computational cells. Droplets with sizes 0.8 μm, 5 μm and 16 μm are exhaled either from a numerical thermal manikin's (NTM) nose or mouth. The spatial distributions of droplets are studied under eight temperature gradients, four heat source configurations and four exhalation modes.

2 Methodology

2.1 Airflow model

The airflow field was modeled by solving the Navier-Stokes equations based on the finite volume method.

$$\frac{\partial(\rho\phi)}{\partial t} + \mathrm{div}(\rho \boldsymbol{U}\phi) = \mathrm{div}\left(\Gamma_\phi \mathrm{grad}\phi\right) + S_\phi \quad (1)$$

Given the complexity of the combined buoyant flow and forced convective flow indoors, the turbulence effect was

taken into account by the renormalization group (RNG) k-ε turbulence model combined with the standard wall function. A discrete ordinates (DO) radiation model was used to consider the radiative heat transfer. Incompressible-ideal-gas law was adopted to reflect the change of air density to temperature in the momentum equations. The convection and diffusion terms for all variables except pressure were discretized by second order upwind and second order central difference scheme, respectively. The pressure term was discretized by Pressure Staggering Option (PRESTO) Scheme. The Semi-Implicit Method for Pressure-Linked Equations (SIMPLE) algorithm was used to couple the pressure and velocity variables. The simulations were carried out with commercially available CFD code FLUENT 12.0.

2.2 Lagrangian particle tracking model

The Lagrangian particle tracking method calculates individual trajectory by solving the particle momentum equation (see Eq. (2)).

$$\frac{\mathrm{d}u_\mathrm{p}}{\mathrm{d}t} = \frac{1}{\tau}\frac{C_\mathrm{D}Re_\mathrm{p}}{24}(u-u_\mathrm{p}) + \frac{g(\rho_\mathrm{p}-\rho)}{\rho_\mathrm{p}} + F_\mathrm{a} \tag{2}$$

For the current study, the additional forces F_a are the sum of Brownian force, thermophoretic force, and the Saffman's lift force. A discrete random walk (DRW) model was used to generate the stochastic velocity fluctuations of the airflow field. The DRW model assumes that the fluctuating velocities follow a Gaussian probability distribution. For isotropic RNG k-ε model, the fluctuating velocity components u' have the following form:

$$u' = \zeta\sqrt{\overline{u'^2}} = \sqrt{2k/3} \tag{3}$$

The Eulerian-Lagrangian scheme is widely used for the study of indoor aerosol dispersion (Chao and Wan 2006; Zhang and Chen 2006; Chen and Zhao 2010). Zhang and Chen (2006) validated the integral performance of the fluid and particle model in indoor application using the experimental data from Mutakami et al. (1992) and from measurements in a under-floor air distribution system. Considering the effect of droplet evaporation, Chen and Zhao (2010) compared their numerical results with two sets of experimental data from Hamey (1982) and Chao and Wan (2006). Generally the numerical model performed well and it is suitable for the study of particle dispersion and distribution in ventilated rooms.

2.3 Particle concentration calculation

Since the Lagrangian method couldn't directly give the particle concentration information, a particle-source-in-cell (PSI-C) sub-routine (Zhang and Chen 2006) was used to correlate the concentration with the Lagrangian particle trajectories in computational cells. The formula of the PSI-C scheme is:

$$\overline{C_j} = \frac{\dot{M}\sum_{i=1}^{n}\mathrm{d}t_{(i,j)}}{V_j} \tag{4}$$

2.4 Evaluation index

Droplets concentration values at a number of locations were used to assess the overall performance of the displacement ventilation system. Besides, the droplet cloud spatial volume (CSV) was used to determine the specific location, shape and size of the indoor polluted zone (Gao et al. 2008). CSV is defined as the spatial volume where the droplet concentration is higher than a fixed value, i.e., the infection threshold of a certain disease. In this study, the infection threshold was set to 10 000 particle/m^3.

3 Case description

A hypothetic office room using displacement ventilation was simulated. The dimensions of the office room are: 4.0 m (length) × 3.0 m (width) × 2.7 m (height) (see Fig. 1). A numerical thermal manikin (NTM) with real body shape was used in order to fully study the effect of its thermal plume. A vertical heat source, a computer and a window were set as other heat sources. The vertical heat source was specially designed to represent the lumped other internal heat sources. Through adjusting its intensity, the vertical air temperature gradient could be changed. The wall, ceiling and floor of the simulated office were assumed to be adiabatic and thus all cooling loads were from internal heat sources. Average temperatures at the outlets were kept at

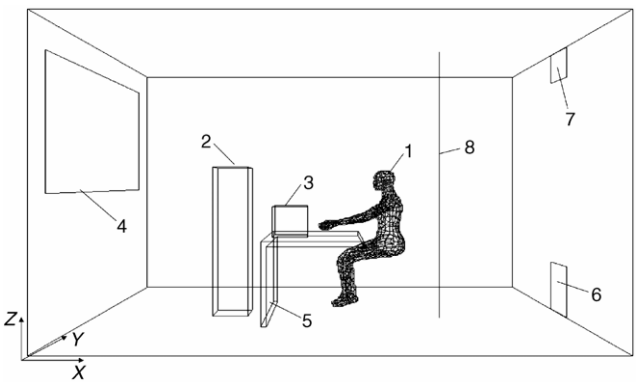

Fig. 1 Configuration of the simulated office (room length (X) 4 m, width (Y) 3 m, height (Z) 2.7 m; 1-numerical thermal manikin (NTM); 2-vertical heat source; 3-computer; 4-window; 5-table; 6-DV inlet 0.4 m × 0.5 m; 7-DV outlet 0.4 m×0.3 m; 8-measuring line)

around 26℃ for all the cases. The air change rate of the room was 5.67 times per hour.

Different thermal conditions that would result in various temperature stratification characteristics and different exhalation modes were studied (see Table 1). From case-1 to case-8, the heat load was increased gradually from 6.25 W to 50.00 W per floor area through adjusting the vertical heat source in order to creat various thermal gradients. For case-7-1 to case-7-6, the heat load was the same as case-7. But in case-7-1, case-7-2 and case-7-3, the configuration of the heat sources was different. In case-7-4, the respiratory flow rate was doubled. In case-7-5 and case-7-6, the air was exhaled from the mouth. The exhalation was 32℃ and at 45° degree downward from the nose or horizontal from the mouth. According to the recent findings on respiratory droplets (Morawska et al. 2009; Chao et al. 2009), we chose to simulate 0.8 μm, 5 μm and 16 μm droplets. The density of the droplets was set as 1000 kg/m^3. The droplet generating rate from the NTM was 100 particles per second.

Due to the stochastic characteristic of the Lagrangian DRW model, it is necessary to test the stabilities of different trajectory numbers. In this study, 328 000 trajectories were found to be sufficient to reach the statistically steady for each droplet size. It is at the same order of the magnitude of the computational cells. A large number of trajectories ensures a more accurate result. But the disadvantage is that it is computationally intensive. In the similar study of indoor particle dispersion, 1000 was used in Zhang and Chen (2006), 5000 in Chen and Zhao (2010), and 49730 in Wan and Chao (2007). Different from previous investigations where the statistical stability for particle concentrations in a very coarse cells (7500 in Zhang and Chen (2006)) or for amounts of deposition at various internal surfaces was emphasized, here calculating the concentration based on the computational cells requires a significantly larger number of particles. The computational time for tracking 328 000 particles was about 2–4 hours on a eight-processor workstation whose CPU's frequency was 3.0 GHz and RAM was 16 GB. The fluid-droplet interaction was assumed as one-way coupling. The initial velocities and temperatures of the droplets were set equal to the exhaled airflows. During droplet tracking, if one droplet reached air supply inlet, outlet, or walls, its trajectory calculation was terminated.

Hybrid mesh scheme was used to generate grid systems. The unstructured tetrahedral meshes were created in the occupied zone of the NTM whereas the hexahedral mesh style was used for the rest of the room. Totally 860 878 cells were used to discretize the computational domain. Grid independence test and model validation of both the flow field and droplet concentration field can be found in Gao et al. (2008, 2009).

4 Results and discussion

4.1 The influence of the temperature gradient

Figure 2 presents the vertical temperature profiles for case-1 to case-8 at the measuring line. Obvious temperature gradients appear in all cases except case-1 where the heat load is too low. The higher the heat load, the steeper the gradient. To investigate the influence of thermal gradient, we deliberately exaggerate the temperature difference in the occupied zone so that in case-4 to case-8 it exceeds the limitation for thermal comfort, i.e., 3℃. The gradients are mainly exists in the occupied zone since the heat sources are all located in the lower part of the room.

Table 1 Case set-up and boundary conditions

Case	Supply air temperature (℃)	NTM (W)	Vertical heat source (W)	Computer (W)	Window (W)	Exhaled condition	Heat load (W/m^2)
Case-1	24.8	75	N/A	N/A	N/A	Nose: 6 L/min 45° downward	6.25
Case-2	23.5	75	75	N/A	N/A	Nose: 6 L/min 45° downward	12.50
Case-3	22.3	75	150	N/A	N/A	Nose: 6 L/min 45° downward	18.75
Case-4	21.0	75	225	N/A	N/A	Nose: 6 L/min 45° downward	25.00
Case-5	19.8	75	300	N/A	N/A	Nose: 6 L/min 45° downward	31.25
Case-6	18.6	75	375	N/A	N/A	Nose: 6 L/min 45° downward	37.50
Case-7	17.3	75	450	N/A	N/A	Nose: 6 L/min 45° downward	43.75
Case-8	16.1	75	525	N/A	N/A	Nose: 6 L/min 45° downward	50.00
Case-7-1	17.3	75	350	100	N/A	Nose: 6 L/min 45° downward	43.75
Case-7-2	17.3	75	200	100	150	Nose: 6 L/min 45° downward	43.75
Case-7-3	17.3	75	250	200	N/A	Nose: 6 L/min 45° downward	43.75
Case-7-4	17.3	75	450	N/A	N/A	Nose: 12 L/min 45° downward	43.75
Case-7-5	17.3	75	450	N/A	N/A	Mouth: 6 L/min horizontal	43.75
Case-7-6	17.3	75	450	N/A	N/A	Mouth: 12 L/min horizontal	43.75

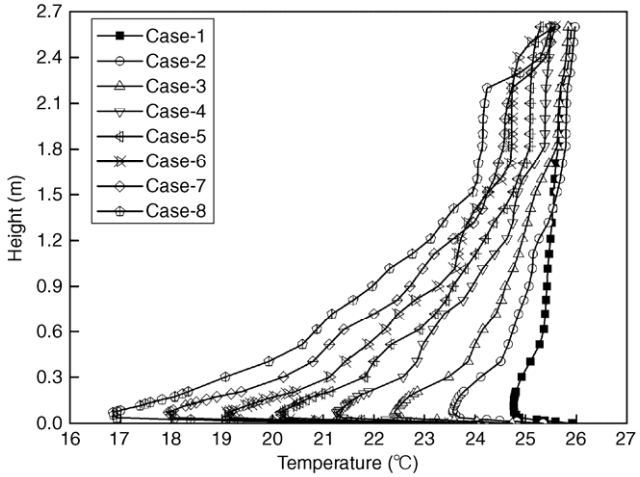

Fig. 2 Vertical temperature profiles at the measuring line (see Fig. 1, item 8)

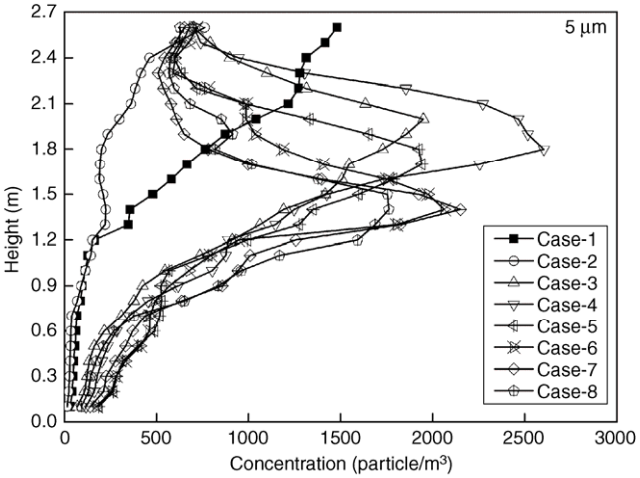

Fig. 4 Average concentrations (5 μm) in planes across the room at different height levels

Figures 3 and 4 show the average values of droplet concentrations of 0.8 μm and 5 μm, individually, in horizontal planes across the room at different heights. From Fig. 3, it is found that the concentration distributions are quite different for the eight cases for 0.8 μm droplets. For case-1 and case-2, the concentration increases monotonically with the height. For case-3 to case-8, a maximum concentration appears in the middle height. The higher the temperature gradient, the lower the maximum concentration would appear. For case-6 to case-8, the maximum concentration appears at about 1.2 m to 1.5 m height (note that the height of the human nose is 1.35 m), which is in agreement with the trap phenomenon found in our previous study (Gao et al. 2008). In case-3, the temperature difference in the occupied zone just reaches the limitation of 3℃. Although the lock-up layer appears the maximum concentration height is fortunately above 1.8 m. It suggests a promising perspective that if the ventilation system is properly designed according to the thermal comfort criteria the trap effect may not be a serious problem. But it should also be noticed that in case-3 the mean concentration in the occupied zone is much higher than in case-1 and case-2. The concentration profiles are almost the same for 0.8 μm and 5 μm.

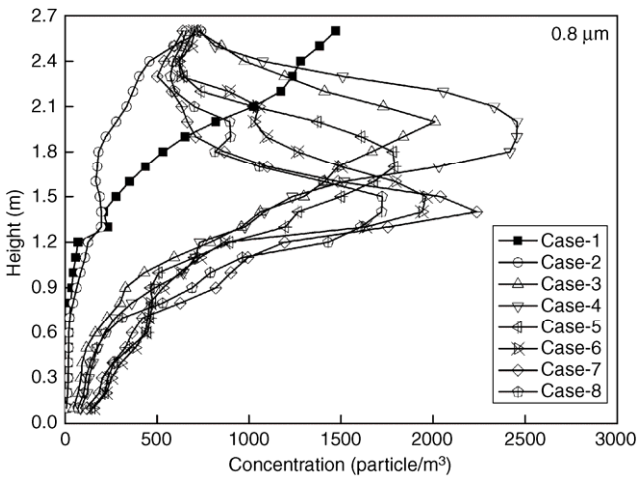

Fig. 3 Average concentrations (0.8 μm) in planes across the room at different height levels

From Fig. 2 to Fig. 4, we can deduce that temperature gradient influence the dispersion of nose exhaled droplets a lot. Figure 5 demonstrates the airflow patterns and temperature distributions in the middle section of the room for case-2, case-4, case-6 and case-8. The temperature stratification from case-2 to case-8 becomes more and more obvious due to the continuous augment of indoor heat load, which agrees with Table 1. It can be seen that the air velocities outside the thermal plumes are very low and the main path for the air to transport to the upper zone is via the natural convections which is in line with the conclusion of Li et al. (2011). It means that if the exhaled air penetrates the thermal plume surrounding the human body and is not entrained by plumes above other heat source it would linger in the space causing a long residence time.

The temperature gradient could influence the NTM's thermal plume in DV systems. The driving force for the upward plume is the temperature difference between the plume and the environment. The temperature gradient strongly influences the height of the plume (Mundt 1995). The steeper temperature gradient results in a weaker thermal plume. In case-2, the thermal plume could reach to the ceiling height. In case-4, the height of the plume is lower and the strength of the plume is weaker than in case-2. In case-8, the steepest gradient severely restrains the development of the plume although the mean temperature in the occupied zone is the lowest.

Figure 6 presents the shape of the droplet cloud spatial volume (CSV) of 0.8 μm droplet. The thermal plume and

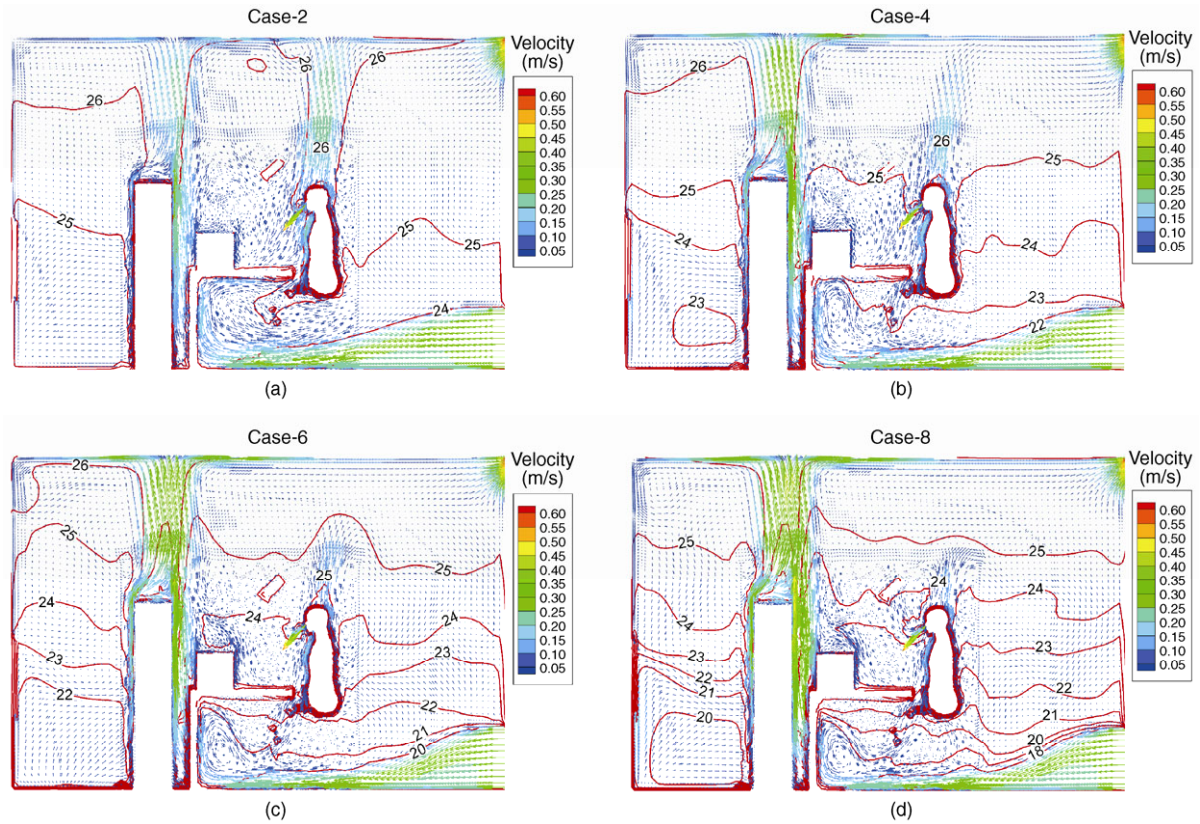

Fig. 5 Airflow patterns and temperature distributions in the middle section of the room ($Y = 1.5$ m) ((a) case-2; (b) case-4; (c) case-6; (d) case-8)

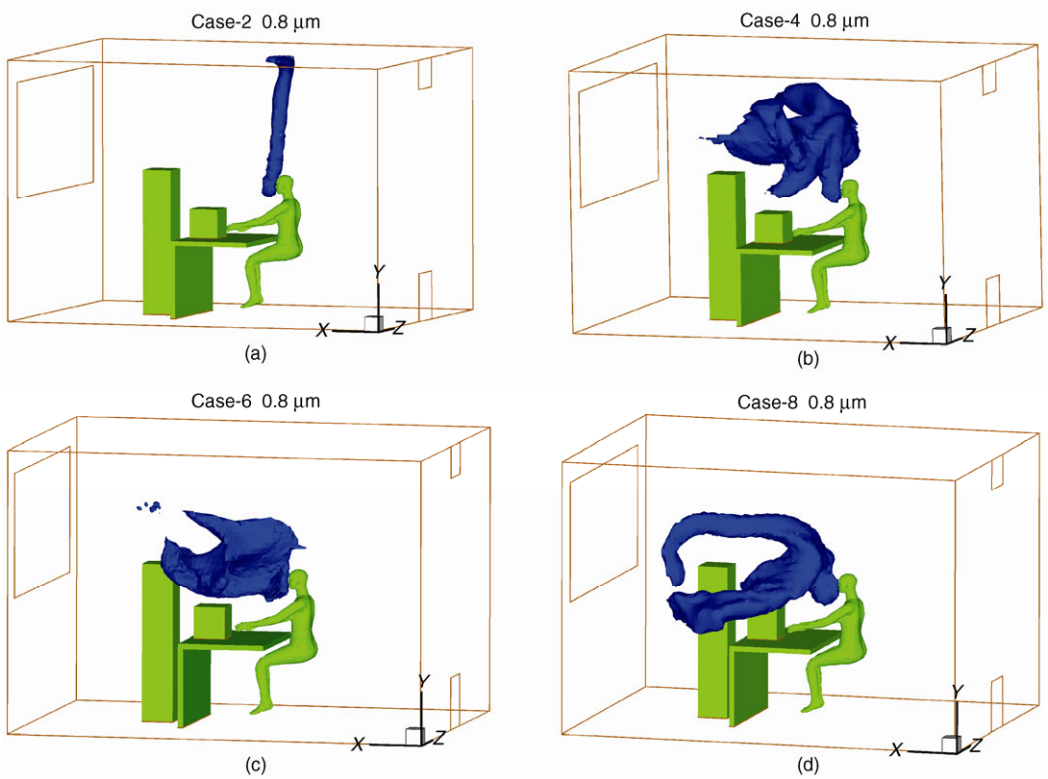

Fig. 6 Shape of the droplet cloud spatial volume (CSV) of 0.8 μm droplet ((a) case-2; (b) case-4; (c) case-6; (d) case-8)

the buoyant exhalation flow are the two ways for the exhaled droplets to transport from the lower zone to the upper zone of the room. For case-1 to case-8, the buoyant exhalation flow from the NTM's nose is too weak and the direction is 45° downward (see Fig. 5), so the thermal plume becomes the main driving force. In Fig. 6(a), the 0.8 μm exhaled droplets could be caught by the NTM's strong plume and be brought to the upper zone which realizes the desired situation expected from DV system. In case-4, the relatively weak thermal plume could bring droplets to a certain height (about 1.8m in this study) and disintegrates at that height. Then the droplets spread horizontally at that height due to temperature stratification. In case-6 and case-8, the NTM's thermal plume couldn't bring the droplets to the upper zone and the trap phenomenon of the exhaled droplets in the breathing zone appears (also see Fig. 3 and Fig. 4). In summary, the effect of temperature gradient is twofold. Firstly it could influence the strength of thermal plume and further the degree of difficulty when the exhalation penetrates the plume. Secondly, it has impact on the horizontal transport (or residence time in the middle height) of the exhaled air after it breaks through the plume.

Figure 7 shows the average values of 16 μm droplet concentrations in horizontal planes across the room at different heights. Because of large gravitational force and more intensive deposition, the maximum concentration is lower than that of 0.8 μm and 5.0 μm. However, in the zone lower than 1.2 m, the mean concentration is even higher than that of 0.8μm and 5.0 μm (especially in case-1 and case-2). It is difficult for the thermal plume to carry 16 μm droplets to the upper zone and the overall upward airflow pattern indoors counteracts the settling of 16 μm droplets. That is why sometimes DV system couldn't perform better than mixing ventilation for removing large droplets. This finding accords to the results of Friberg et al. (1996) and our previous finding using Eulerian drift-flux method (He et al. 2011).

4.2 The influence of the heat source configuration

In case-7-1, case-7-2 and case-7-3, the computer near the NTM is turned on. The difference between case-7-1 and case-7-2 is whether there is a heat source in the upper zone of the room. The difference between case-7-1 and case-7-3 is the intensity of the computer heat source. The vertical temperature profiles for case-7, case-7-1, case-7-2 and case-7-3 at the measuring line are almost the same (the figure is not presented here). This finding agrees with that the temperature gradient in a room with DV is not so much dependent on the configuration of the heat sources (Mundt 1995). However, the strong heat source near the NTM can influence the dispersion of the exhaled droplets. The droplets profiles are similar for case-7, case-7-1, case-7-2 and case-7-3 (see Fig. 8) but the maximum concentration values are decreasing with the increasing of the heat source (the computer) near the NTM. Although the trap phenomenon still exists in the four cases, the strong heat source near the NTM could help transport the small exhaled droplets to the upper zone.

For 16 μm droplets, the strong heat source near the NTM could slightly reduce the maximum concentrations, as shown in Fig. 9. The thermal plume has relatively smaller influence on 16 μm droplets due to their large gravitational force.

4.3 The influence of the exhalation mode

In this section, the effect of the exhalation modes on the dispersion of exhaled droplets is analyzed. The pulmonary ventilation is about 5–6 L/min for a person at rest and can

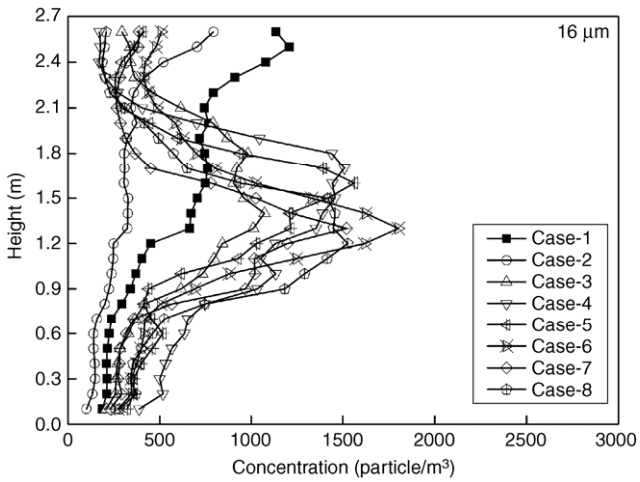

Fig. 7 Average concentrations (16 μm) in planes across the room at different height levels (case-1 to case-8)

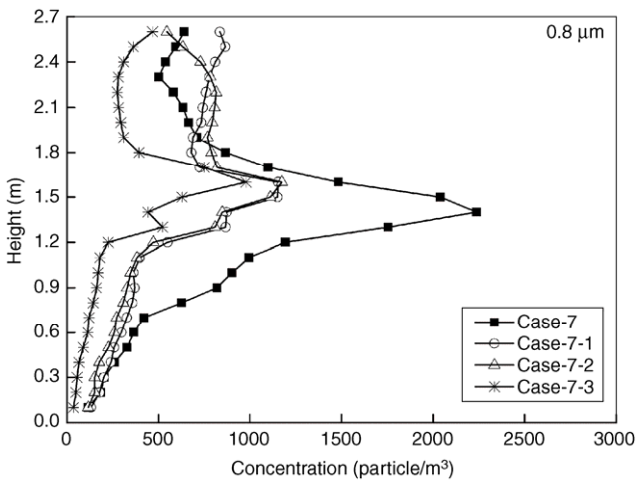

Fig. 8 Average concentrations (0.8 μm) in planes across the room at different height levels

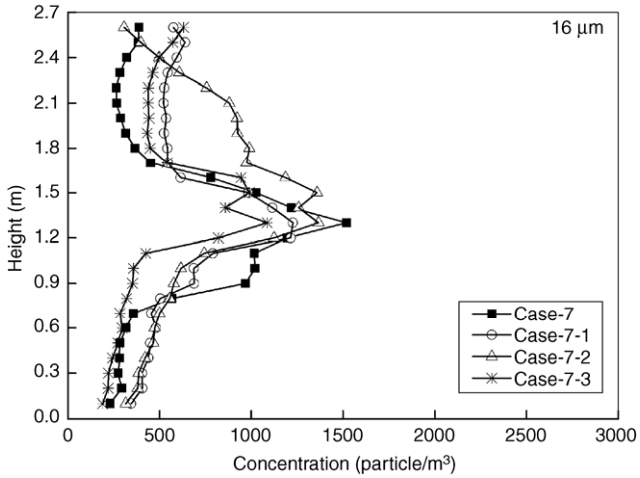

Fig. 9 Average concentrations (16 μm) in planes across the room at different height levels

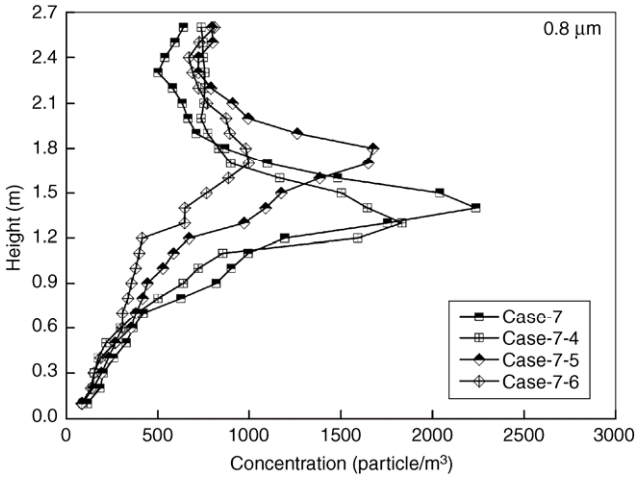

Fig. 10 Average concentrations (0.8 μm) in planes across the room at different height levels

reach up to 20 times higher depending on the metabolism (Bjorn and Nielsen 2002). In this study, we set the four exhalation modes mainly based on the office work condition. It is observed in Fig. 10 that no matter exhalation through mouth or nose, a maximum concentration appears in the middle height. The location of maximum concentration in the nose mode is slightly lower than in the mouth mode due to counteraction between the 45° downward exhaled flow and the upward buoyant flows.

Another finding is that in the lock-up layer is higher for the case of 6 L/min exhalation. The shapes of the droplet CSV for 0.8 μm droplet of the four cases (see Fig. 11) may explain it. For the larger exhalation flow rates (case-7-4 and case-7-6), the CSVs are smaller and the CSVs mainly gather at the core region of the exhalation flow. For the smaller exhalation flow rates (case-7 and case-7-5), the droplets disperse quickly after they are generated and the CSVs are larger.

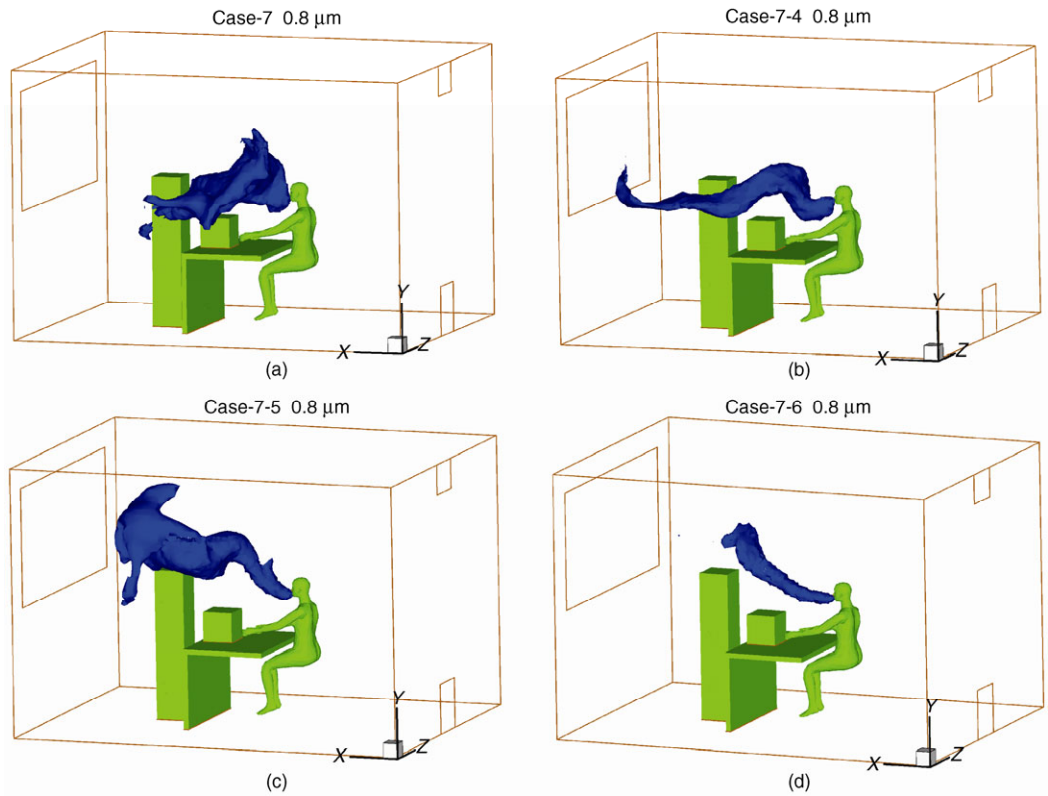

Fig. 11 Shape of the droplet cloud spatial volume (CSV) of 0.8 μm droplet ((a) case-7; (b) case-7-4; (c) case-7-5; (d) case-7-6)

For 16 μm droplets, the features for 0.8 μm also present (see Fig. 12). However, as in Fig. 7 and Fig. 9, the differences among the cases are not so remarkable. That is, the influence of air flow pattern on the concentration distributions is not as significant as small particles and gaseous pollutants.

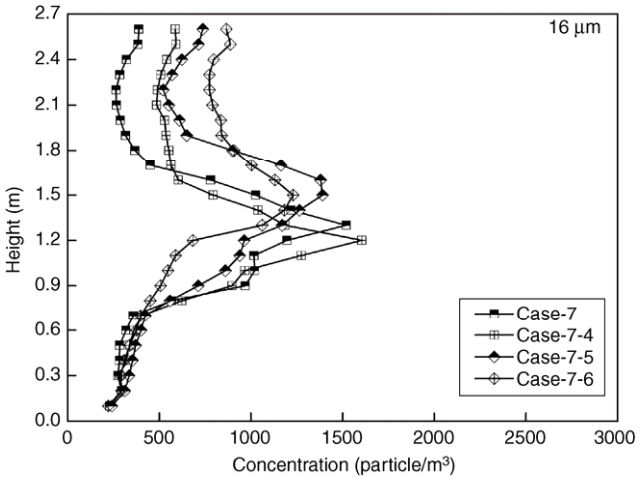

Fig. 12 Average concentrations (16 μm) in planes across the room at different height levels

5 Conclusions

This paper studies the lock-up (or trap) phenomenon of human exhaled droplets in the stratified environment. The following conclusions may be drawn:

(1) Large temperature gradient would result in the trap phenomenon of exhaled droplets (smaller than 5 μm) in the breathing height. This is because large temperature gradient would restrain the development of the NTM's thermal plume and extend the residence time of droplets in the occupied zone.

(2) The strong heat source near the NTM could help to transport the small droplets to the upper zone and decrease the concentration value in the trapped zone.

(3) Both nose-exhaled and mouth-exhaled small droplets would be trapped at the breathing height if the temperature gradient is sufficiently large whereas the trap height for the mouth mode is a little higher.

(4) The large gravitational force of 16 μm counteracts the overall upward airflow in DV which may result in a higher concentration in the occupied zone. Airflow pattern and thermal stratification do not influence their concentrations as significant as for 0.8 μm and 5.0 μm droplets.

In this study the air change rate does not change. In practice, for VAV systems, the supply airflow rate may be regulated according to the loads. Thus the ambient indoor air velocity level changes accordingly. The lock-up phenomenon is this situation requires further studies. Besides, the heat flux of body surface is set to be constant. However, the heat flux and the surface temperature may vary with the environment. The natural convection of occupants with inner-body thermoregulation model will be helpful to characterize the plume in a more realistic way.

Acknowledgements

This study was financially supported by the National Natural Science Foundation of China under the project No. 50808133, the Research Grant Committee, Hong Kong, China, under the project No. RGC GRF 526508, and the Fundamental Research Funds for the Central Universities.

References

Bjorn E, Nielsen PV (2002). Dispersal of exhaled air and personal exposure in displacement ventilated rooms. *Indoor Air*, 12: 147 – 164.

Brohus H, Nielsen PV (1996). Personal exposure in displacement ventilated rooms. *Indoor Air*, 6: 157 – 167.

Chen C, Zhao B (2010). Some questions on dispersion of human exhaled droplets in ventilation room: answers from numerical investigations. *Indoor Air*, 20: 95 – 111.

Chao CYH, Wan MP (2006). A study of the dispersion of expiratory aerosols in unidirectional downward and ceiling-return type airflows using a multiphase approach. *Indoor Air*, 16: 296 – 312.

Chao CYH, Wan MP, Morawska L, Johnson GR, Ristovski ZD, Hargreanes M, Mengersen K, Corbett S, Li Y, Xie X, Katoshevski D (2009). Characterization of expiration air jets and droplet size distributions immediately at the mouth opening. *Journal of Aerosol Science*, 40: 122 – 133.

Chao CYH, Wan MP, To GNS (2008). Transport and removal of expiratory droplets in hospital ward environment. *Aerosol Science and Technology*, 42: 377 – 394.

Friberg B, Friberg S, Burman LG, Lundholm R, Ostensson R (1996). Inefficiency of upward displacement operating theatre ventilation. *Journal of Hospital Infection*, 33: 263 – 272.

Gao N, Niu J, Morawska L (2008). Distribution of respiratory droplets in enclosed environments under different air distribution methods. *Building Simulation*, 1: 326 – 335.

Gao NP, Niu JL, Perino M, Heiselberg P (2009). The airborne transmission of infection between flats in high-rise residential buildings: Particle simulation. *Building and Environment*, 44: 402 – 410.

Hamey PY (1982). The evaporation of airborne droplets. Msc Thesis, Bedford-shire, UK, Granfield Institute of Technology, 48 – 58.

Han K, Zhu XP, He F, Liu LG, Zhang LJ, Ma HL, Tang XY, Huang T, Zeng G, Zhu BP (2009). Lack of Airborne Transmission during Outbreak of Pandemic (H1N1) 2009 among Tour Group Members, China, June 2009. *Emerging Infectious Diseases*, 15: 1578 – 1581.

He Q, Niu J, Gao N, Zhu T, Wu J (2011). CFD study of exhaled droplet transmission between occupants under different ventilation strategies in a typical office room. *Building and Environment*, 46: 397 – 408.

Li Y, Nielsen PV, Sandberg M (2011). Displacement ventilation in hospital environments. *ASHRAE Journal*, 53: 86 – 88.

Mangili A, Gendreau MA (2005). Transmission of infectious diseases during commercial air travel. *Lancet*, 365: 989 – 996.

Morawska L, Johnson GR, Ristovski ZD, Hargreaves M, Mengersen K, Corbett S, Chao CYH, Li Y, Katoshevski D (2009). Size distribution and sites of origin of droplets expelled from the human respiratory tract during expiratory activities. *Journal of Aerosol Science*, 40: 256 – 269.

Mundt E (1995). Displacement ventilation systems—Convection flows and temperature gradients. *Building and Environment*, 30: 129 – 133.

Mui KW, Wong LT, Wu CL, Lai ACK (2009). Numerical modeling of exhaled droplets nuclei dispersion and mixing in indoor environments. *Journal of Hazardous Materials*, 167: 736 – 744.

Murakami S, Kato S, Nagano S, Tanaka S (1992). Diffusion characteristics of airborne particles with gravitational settling in a convection-dominant indoor flow field. *ASHRAE Transaction*, 98(1): 82 – 97.

Nicas M, Nazaroff WW, Hubbard A (2005). Toward understanding the risk of secondary airborne infection: Emission of respirable pathogens. *Journal of Occupational and Environmental Hygiene*, 2: 143 – 154.

Nielsen PV, Olmedo I, Adana MR, Grzelecki P, Jensen RL (2012). Airborne cross-infection risk between two people standing in surroundings with a vertical temperature gradient. *HVAC & R Research*, in press. DOI: 10.1080/10789669.2011.598441.

Qian H, Li Y, Nielsen P, Hyldgaard C, Wong T, Chwang A (2006). Dispersion of exhaled droplet nuclei in a two-bed hospital ward with three different ventilation systems. *Indoor Air*, 16: 111 – 128.

Seepana S, Lai ACK (2012). Experimental and numerical investigation of interpersonal exposure of sneezing in a full-scale chamber. *Aerosol Science and Technology*, 46: 485 – 493.

Skistad H, Mundt E, Nielsen PV, Hagstrom K, Railio J (2004). Displacement ventilation in non-industrial premises. Brussels: Rehva.

Wagner BG, Coburn BJ, Blower S (2009). Calculating the potential for within-flight transmission of influenza A (H1N1). *BMC Medicine*, 7: 81.

Wan MP, Chao CYH (2007). Transport characteristics of expiratory droplets and droplets nuclei in indoor environments with different ventilation airflow patterns. *Journal of Biomechanical Engineering*, 129: 341 – 353.

Zhang Z, Chen Q (2006). Experimental measurements and numerical simulations of particle transport and distribution in ventilated rooms. *Atmospheric Environment*, 40: 3396 – 3408.

Zhao B, Zhang Y, Li X, Yang X, Huang D (2004). Comparison of indoor aerosol particle concentration and deposition in different ventilated rooms by numerical method. *Building and Environment*, 39: 1 – 8.